마이크로머쉰의 자동 시뮬레이션 시스템

Automated Simulation System for Micromachines

이 준 성*
Lee, Joon-Seong

Abstract

This paper describes a new automated simulation system for micromachines whose size range 10^{-6} to 10^{-3} m. An automatic finite element (FE) mesh generation technique, which is based on the fuzzy knowledge processing and computational geometry technique, is incorporated into the system, together with one of commercial FE analysis codes, MARC, and one of commercial solid modelers, Designbase. The system allows a geometry model of concern to be automatically converted to different FE models, depending on physical phenomena of micromachines to be analyzed, i.e. electrostatic analysis, stress analysis, modal analysis and so on. The FE models are then automatically analyzed using the FE analysis code. Among a whole process of analysis, the definition of a geometry model, the designation of local node patterns and the assignment of material properties and boundary conditions onto the geometry model are only the interactive processes to be done by a user. The interactive operations can be processed in a few minutes. The other processes which are time consuming and labour-intensive in conventional CAE systems are fully automatically performed in a popular engineering workstation environment. This automated simulation system is successfully applied to evaluate an electrostatic micro wobble actuator.

Key words : Micromachine, Fuzzy Knowledge Processing, Computational Geometry, Finite Element Analysis, Micro Wobble Actuator

1. Introduction

Nuclear structural components such as pressure vessels and piping are typical examples of huge scale artifacts, while micromachines are typical examples of tiny scale artifacts. Micromachines are extremely novel artifacts with a variety of special characteristics. Utilizing their tiny dimensions ranging roughly from 10^{-6} to 10^{-3} m, the micromachines can perform tasks in a revolutionary manner that would be impossible for conventional artifacts [1]. Designing microma-

* 경기대학교 기계공학과

chines is (a) multi-disciplinary, (b) strongly interactive among design subprocesses such as design specification, conceptual design and detail design, (c) it also requires designers living in the macroscopic world to have very different empirical knowledge being valid in the microscopic world. Micromachines are in general related to various coupled physical phenomena. They are required to be evaluated and designed considering the coupled phenomena. A lot of trial and error evaluations are indispensable. Such situations make it very difficult to find a satisfactory or optimized solution of micromachines, although numerous optimization algorithms have been studied.

In accordance with dramatical progress of computer technology, numerical simulation methods such as the finite element method (FEM) are recognized to be key tools in practical designs and analyses. Computer simulations allow for the testing of new designs and for the iterative optimization of existing designs without time-consuming and considerable efforts to experiments at every iteration process. Especially, computer simulation seems essential for micromachine design, since it is often very difficult to precisely measure physical phenomena in the microscopic world. However, conventional computational analyses of micromachines are still labour-intensive and are not easy for ordinary designers and engineers to perform. It is difficult for them to find a satisfactory or optimized solution of micromachines, utilizing such conventional computer simulations tools.

Some CAD (Computer-Aided Design) / CAE (Computer-Aided Engineering) systems for micromachines such as SENSIM [2], FastCap [3], MEMCAD [4] and CAEMEMS [5] have been developed so far. SENSIM allows for the modeling of silicon piezoresistive or capacitive pressure sensors of multiple thin films, and for the calculation of their stress and deflection as a function of both pressure and temperature using both analytical and finite difference solutions under a thermoelastic plane stress conditions. FastCap is a boundary element analysis program for three-dimensional electrostatic capacitance, which was used to efficiency analyze capacitance-driven micromachines. MEMCAD is an integrated CAD system consisting of a structure generation software, FastCap, one of commercial solid modelers Pro/Engineer, one of commercial finite element (FE) codes ABAQUS, and specialized database. This system can perform both mechanical and electrical analyses of structures either described directly, or derived from the design specification (mask data plus process flow). CAEMEMS has a capability of parametric modeling of devices, and employs one of commercial FE codes ANSYS. One module of CAEMEMS is specially developed for diaphragm of pressure sensors. In these systems, FE codes to simulate behaviors of micromachines play very important roles. To more improve efficiency of design processes of actual micro structures with arbitrary geometry shape, it is indispensable to fully automate FE modeling and analyses of them.

The present author has proposed an automatic FE mesh generation method for three-dimensional complex geometry [6]. The author has integrated this mesh generator, one of commercial FE analysis codes MARC [7] and one of commercial solid modelers Designbase [8] into a novel simulation system for micromachines. This simulation system includes the following functions ; (a) definition of geometry model, i.e. solid modeling including boolean operations such as union and intersection and easy formation of free-form surfaces, (b) attachment of boundary conditions and material properties directly to geometry model, (c) fully automated mesh generation, (d) various FE analyses such as electrostatic, stress and modal analyses, and (e) visualization of analysis models and results.

The developed system is applied to evaluate one of electrostatic micro wobble actuators [9]. Through the analyses, fundamental performances of the system are cleary demonstrated.

2. Outline of the System

The developed simulation system allows designers to evaluate detailed physical behaviors of micromachines through some simple interactive operations to their geometry models. In other words, designer do not have to directly deal with mesh data when they operate this simulation system. A

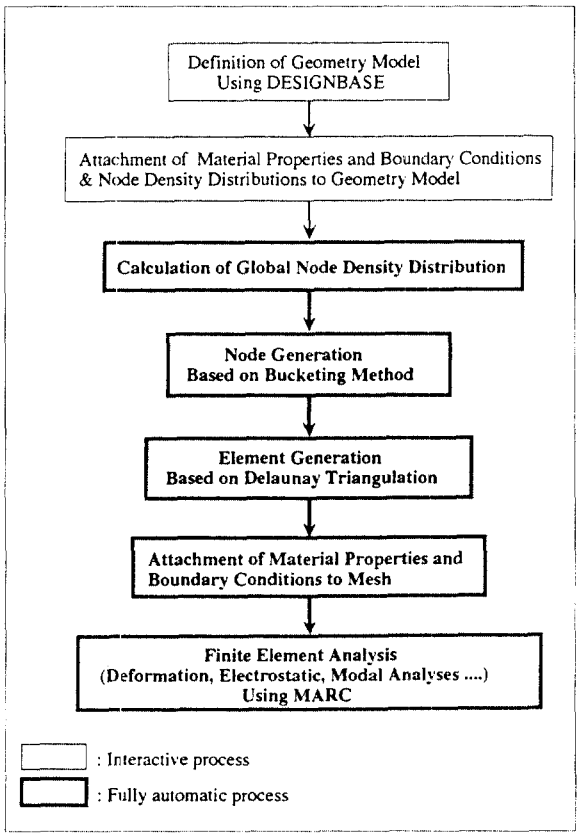

〈Fig 1〉 Flow of analysis

flow of analyses using the system is shown in 〈Fig 1〉. Each subprocess will be described below. The details of the mesh generation part can be found elsewhere [6].

2.1 Definition of Geometry Model

A whole analysis domain is defined using one of commercial geometry modelers, Designbase [8], which has abundant libraries enabling us to easily operate, modify and refer to a geometry model. Any information related to a geometry model can be easily retrieved using those libraries. It should be noted here that different geometry models are constructed, depending on physical behaviors to be analyzed. In these modelers, three-dimensional geometric data are stored as a tree structure of domain-surface (free-form surfaces such as Bezier or Gregory type surfaces)-edge (B-spline or Bezier type curves)-vertices.

2.2 Attachment of Material Properties and Boundary Conditions to Geometry Model

Material properties and boundary conditions are directly attached onto the geometry model by clicking the loops or edges that are parts of the geometry model using a mouse, and then by inputting actual values. The present system accepts Direchlet's and Neumann's type boundary conditions.

2.3 Designation of Node Density Distributions

In the present system, nodes are first generated, and then an FE mesh is built. In general, it is difficult to well control element size for a complex geometry. A node density distribution over a whole geometry model is constructed as follows.

The present system stores several local nodal patterns such as the pattern suitable to well capture stress concentration, the pattern to subdivide a finite domain uniformly, and the pattern to subdivide a whole domain uniformly. A user selects some of those local node patterns, depending on their analysis purposes, and designates their relative importance and where to locate them. The process is illustrated in 〈Fig 2〉, taking an upper half portion of a single cracked plate with holes as an example. For example, when either the crack or the hole exists solely in an infinite domain, the local node patterns for stress concentration may be regarded locally-optimum around the crack-tip or the hole. When these stress concentration sources exist closely to each other in the analysis domain, extra nodes have to be removed from the superposed region of both patterns. In the present method, a global distribution of node density over the whole analysis domain is automatically calculated through their superposition using the fuzzy knowledge processing [10,11] as shown in 〈Fig 2〉 (c), (d). When designers do not want any special meshing, they can adopt uniformly subdivided mesh.

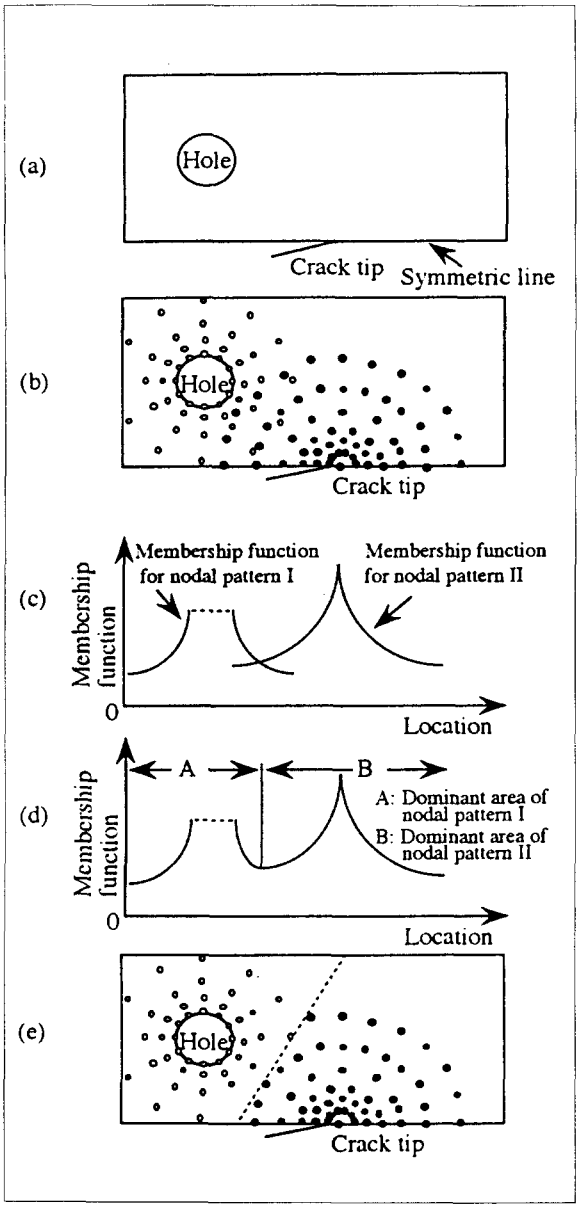

〈Fig 2〉 Superposition of nodal patterns based on fuzzy theory

2.4 Node and Element Generation

Node generation is one of time consuming processes in automatic mesh generation. Here, the bucketing method [12] is adopted to generate nodes which satisfy the distribution of node density over a whole analysis domain. 〈Fig 3〉 shows its fundamental principle, taking the previous two-dimensional mesh generation as an example without any loss of generality. Let us assume that the distribution of node density over a whole analysis domain is already given as shown in 〈Fig 3〉(a). At first, a super-rectangle enveloping the analysis domain is defined as shown in 〈Fig 3〉(b). In the three-dimensional solid case, a super hexahedron is utilized to envelop an analysis domain. Next, the super-rectangle is divided into a number of small sub-rectangles, each of which is named "Bucket" Nodes are generated bucket by bucket.

At first, a number of candidate nodes with uniform spacing are prepared in one of buckets as shown in 〈Fig 3〉(c). The distance of two neighboring candidate nodes is set to be smaller than the minimum distance of nodes to be generated in the relevant bucket. Next, candidate nodes are pick up one by one, starting from the left-bottom corner of the bucket, and are put into the bucket. A candidate node is adopted as one of the final nodes when it satisfies the following two criteria :

(a) The candidate node is inside the analysis domain (IN/OUT check).

(b) The distance between the candidate node and the nearest node already generated in the bucket satisfies the node density at the point to some extent.

Practically, the criterion (a) is first examined bucket by bucket.. As for buckets lying across the domain boundary, the criterion (a) is examined node by node. It should be noted here that the nodes already generated in the neighboring buckets have to be examined for the criterion (b) as well when a candidate node is possibly generated near the border of the relevant bucket. Thanks to the bucketing method, the number of examinations of the criterion (b) can be reduced significantly, and then a node generation speed is remained to be proportional to the total number of nodes. As for three-dimensional solid geometries, nodes are generated in the following order : vertices, edges, surfaces and domain.

The Delaunay triangulation method [13,14] is utilized to

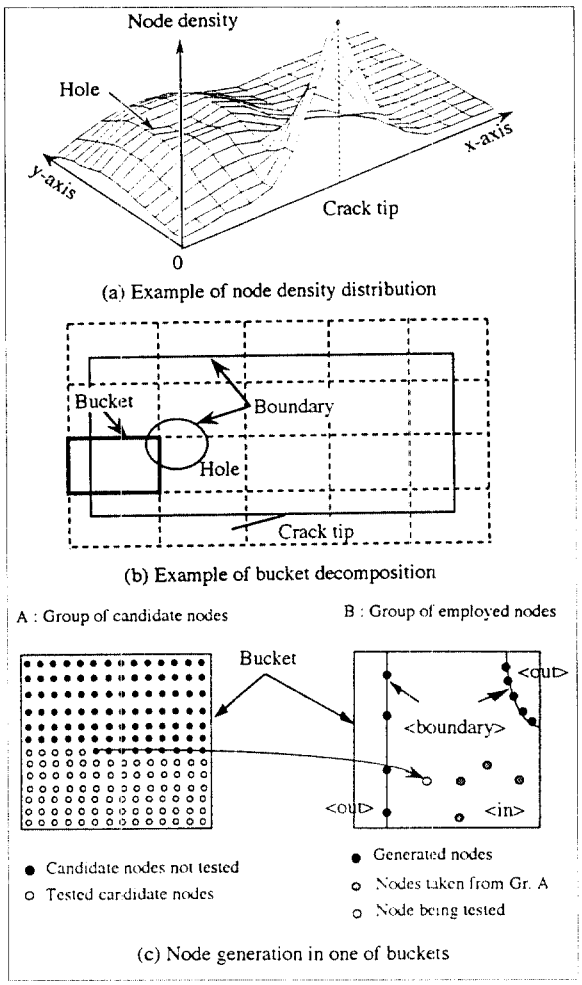

〈Fig 3〉 Node generation based on bucketing method

generate tetrahedral elements from numerous nodes given in a geometry. The speed of element generation by the Delaunay triangulation method is proportional to the number of nodes. If this method is utilized to generate elements in a geometry with indented shape, elements are inevitably generated even outside the geometry. However, such mis-match elements can be removed by performing the IN/OUT check for gravity center points of such elements.

2.5 Attachment of Material Properties and Boundary Conditions to FE Mesh

Through the interactive operations mentioned in section 2.2, a user designates material properties and boundary conditions onto the geometry model. Then these are automatically attached onto appropriate nodes, edges, faces and volume of elements. Such automatic conversion can be performed owing to the special data structure of finite elements such that each part of element knows which geometry part it belongs to. Finally, a complete FE model consisting of mesh, material properties and boundary conditions is created.

2.6 FE Analyses

The present system automatically converts a geometry model of concern to various FE analysis models, depending on physical phenomena to be analyzed, i.e. stress analysis, modal analysis, thermal conduction analysis, electrostatic analysis, and so on. The current version of the system produces FE models of quadratic tetrahedral elements, which are compatible to one of commercial FE codes, MARC [7]. Then FE analyses are automatically performed. FE models and FE analyses results are visualized using a pre/post processor of MARC, MENTAT [7].

3. Electrostatic Micro Wobble Actuator

The developed simulation system is applied to one of electrostatic micro wobble actuators [9]. Despite a large number of electrostatic motor designs [15], few large-scale electrostatic actuators are in use. In a microscopic domain, an electrostatics mechanism appears to be more advantageous to use [16]. A number of efforts have been made so far to build electrostatic micro actuators [17-22]. However, most of the micro actuators have failed to generate enough force for practical applications. Therefore, a new concept of micro actuator is demanded. The micro actuator considered in the present study is designed as a part of a positioning device

[9]. This actuator uses an electrostatic force as other micro-actuators do, and its fabrication process using the silicon technology is almost the same as those in refs. [18,21]. Compared to similar devices the micro actuator named "wobble actuator" has several advantages such as high performance, high reliability and high productivity.

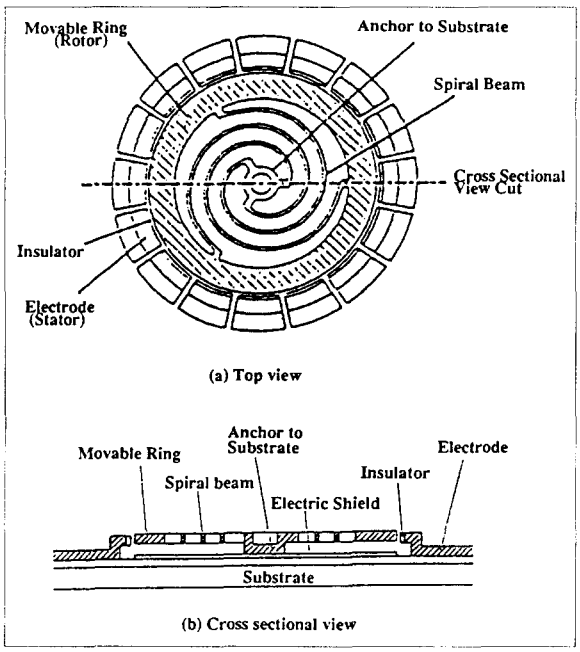

〈Fig 4〉 Basic structure of micro wobble actuator

The basic structure of the micro wobble actuator is shown in 〈Fig 4〉. 〈Fig 4〉(a) shows its schematic plane view, while 〈Fig 4〉(b) does its cross-section view. The micro actuator comprises a movable platform, i.e. rotor, three spiral beams, and a plurality of electrodes, i.e. stator. Dimensions of its initial design are as follows. The platform is a ring-like plate of approximately 200 μm in outer diameter and 150 μm in inner diameter. The three beams are disposed at the inner space of the ring, and connect the ring with a substrate. The electrodes are provided in the circumferential region around the platform by about 3 μm to play the same role as ordinary electrostatic micro actuators. Insulator of about 1 μm thick is coated in inner surfaces of electrodes. As each electrode is excited sequentially, the ring rolls inside of the electrodes, accompanied by a little distortion of the three spiral beams. When the ring rolls around the electrodes in one cycle without slipping, it has transversed a distance greater than its own circumference. The driving force produced as an electrostatic attraction force is generated between the two bodies, i.e. the ring and each electrode. Although the rotation of the ring is limited by the spiral beams, the present actuator has several advantages such as high torque and low friction. Particular dimensions of the actuator are shown in 〈Table 1〉. Material properties of silicon are summarized in 〈Table 2〉.

Table 1 Reference dimensions

Diameter of Plane Ring	200 μm
Thickness of Plame Ring	2.5 μm
Inner Diameter of Electrodes	206 μm
Thickness of Spiral Beams	2.5 μm
Width of Spiral Beams	5.0 μm
Angle of Spiral Beams	360deg.
Thickness of Insulator	1.0 μm

Table 2 Material properties

Material	Si
Young's modulus	190 GPa
Poisson's ratio	0.3
Yield stress	7GPa
Mass density	2300 kg/m^3
Permittivity of Insulator	4.0

4. Results and Discussions

Let us examine a fundamental capability of the developed automated simulation system. To examine mechanical and electrostatic feasibility of the present micro wobble actuator, the following behaviors have to be evaluated.

(1) In-plane deformation of the rotor portion, i.e. the ring with the three spiral beams, caused due to an electrostatic

force.

(2) Out-of-plane deformation of the rotor portion caused due to its weight.

(3) Modal analysis of the rotor portion

(4) Electrostatic analysis of the air gap between the ring and one of the electrodes.

(5) Recovery process of the deformed rotor portion.

In general, it is an extremely time-consuming work to perform all the analyses alone. However, they can be done very easily by using the developed simulation system. Assuming the reference configuration and material properties given in 〈Table 1〉 and 〈Table 2〉, the above phenomena are analyzed. The results are described below.

4.1 In-plane Deformation of Rotor

In-plane deformation of the rotor portion is analyzed to evaluate the quantitative relationship between a rotation angle ϕ and a torque τ, necessary to rotate the rotor within the elastic limit of the beams. 〈Fig 5〉 illustrates boundary conditions of the present analysis. In reality, the rotor is attracted to contact with one of the electrodes through an electrostatic force. In this analysis, the displacement-controlled force with the magnitude of the distance between the rotor and one of the electrodes is applied to the rotor, considering its rotation along the inner surface of the electrodes for the purpose of simplicity. Since the electrode is much stiffer than the spiral beam, the in-plane deformation of the electrode is negligible. Thus the simplification of the loading condition employed here is quite reasonable.

〈Fig 6〉 shows a geometry model of the rotor portion, while 〈Fig 7〉 illustrates a typical FE mesh, which consists of 24,655 tetrahedral quadratic elements and 50,583 nodes. Through some preliminary analyses, this mesh is selected to give us an almost converged result of global behavior of the rotor. Flow chart of the deformation analysis is shown in 〈Fig 8〉. 〈Fig 9〉 shows a calculated distribution of equivalent stress at rotation angle ϕ of 62 degrees at which the deformation reaches the elastic limit of Si, i.e. 7 GPa. The maximum stress occurs near the internal dent part of one

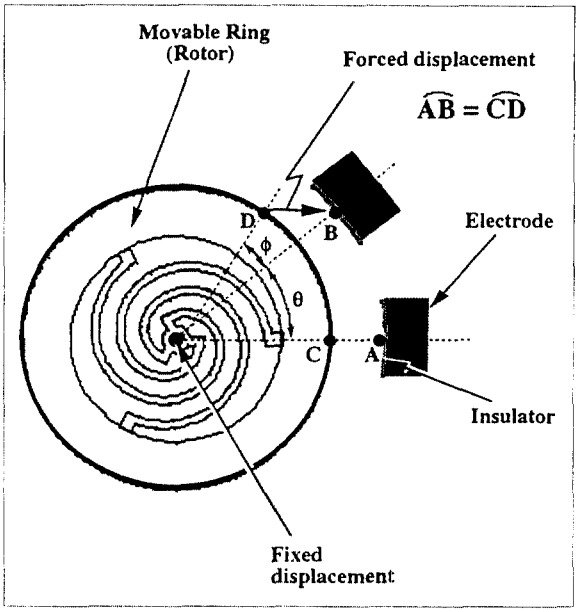

〈Fig 5〉 Boundary conditions for in-plane deformation analysis of rotor

beam and, as anticipated, at a junction part of other beam. The ring itself does not deform much. The detailed shape of the junction may have to be manufactured very carefully in order to avoid dangerous stress concentration. 〈Fig 10〉 shows the relationship between the calculated torque τ and the rotation angle ϕ. It can be seen from the figure that the rotation of the rotor is limited at about 62 degrees because of the elastic limit. 〈Fig 10〉 also indicates that the starting torque τ_0 required is 0.42 x 10^{-9} Nm. This value of the starting torque will be referred to in the section of electrostatic analyses.

4.2 Out-of-plane Deformation of Rotor due to Its Weight

Since the width of the rotor is very thin compared to its diameter, i.e. 2.5 μm vs. 200 μm, the out-of-plane deformation of the rotor was analyzed using the same FE mesh shown in 〈Fig 7〉. The maximum deflection calculated

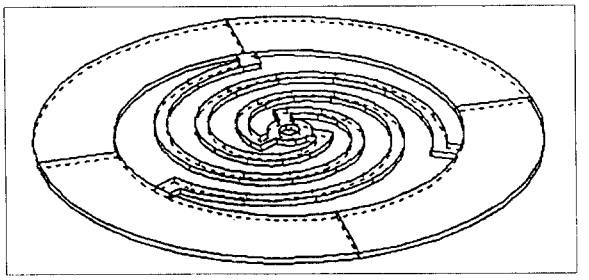

〈Fig 6〉 Geometry model of rotor

〈Fig 7〉 FE mesh of rotor(No. of elements=24,655,No. of nodes=50,583)

was 2.049 × 10^{-5} μm. This value is negligible compared with the in-plane deformation of the rotor. Such a high stiffness of a thin structure is one of typical scaling effects of micro structures.

4.3 Modal Analysis of Rotor

Using the same mesh as in 〈Fig 7〉, modal analyses of the rotor were performed to examine its dynamic performance. 〈Fig 11〉 shows the calculated first and second eigen modes

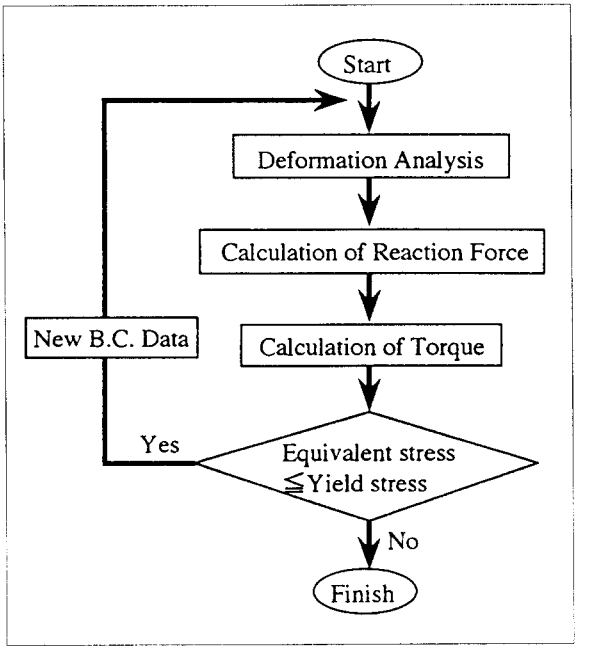

〈Fig 8〉 Flow chart of the deformation analysis

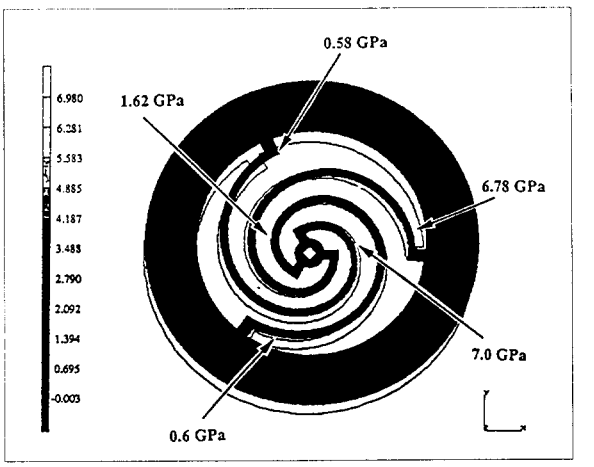

〈Fig 9〉 Calculated distribution of equivalent stress(ϕ=62 degress)

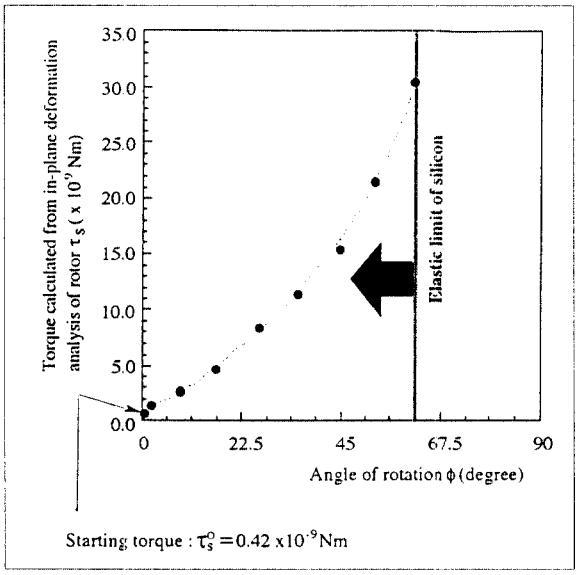

〈Fig 10〉 Calculated torque vs. rotation angle

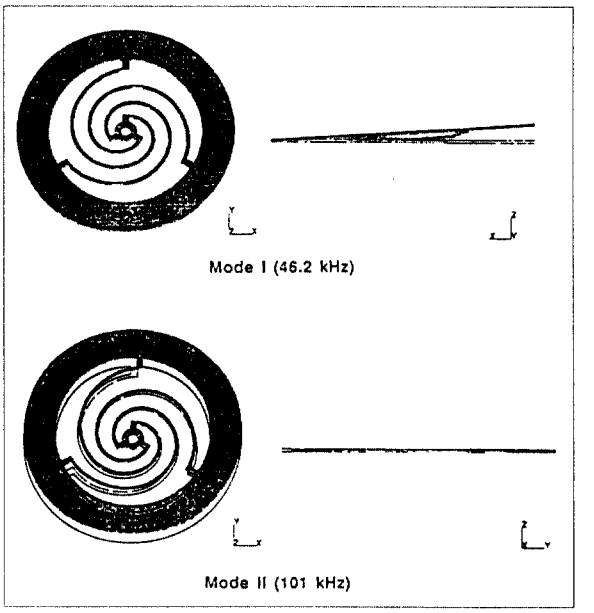

〈Fig 11〉 Calculated first and second eigen modes of rotor

with eigen frequencies. The calculated first eigen frequency is 46 kHz, which is far beyond the minimum requirement of 10 kHz for a micro-positioner.

4.4 Electrostatic Analysis of Air Gap between Rotor and Stator

In general, to estimate electrostatic performances of micro actuators, in-plane 2D FE analyses are often conducted because of the complexity of actual micro actuator geometry. Here, an actual 3D geometry of micro actuator is considered in order to take account of electrical leakage phenomena. 〈Fig 12〉 shows a geometry model and boundary conditions of an upper part of the air gap between the rotor and the stator. Here a sufficiently large area of the air was modeled in order to approximately take into account infinite boundary conditions. As material properties, the permittivity of the air and insulator of SiO_2, were assumed to be 8.854 x 10^{-12} C/Vm and 3.542 x 10^{-11} C/Vm, respectively.

When one of the electrodes is excited, the rotor will be electrostatically attracted and come to contact with the insulator on the inner surface of the electrode. Then as this electrode is discharged and voltage is supplied to the next electrode, the rotor will revolve, being attracted by the excited electrode. At this moment, potential energy is stored in the capacitor formed by the rotor and the excited electrode.

Flow chart of the electrostatic analysis is shown in 〈Fig 13〉. 〈Fig 14〉 shows the calculated curves of starting torque τ_e^0 vs. driving voltage V. Here, a solid curve denotes the 3D FE solutions, while the broken curve does 2D analytical solutions [23]. It can be seen from this figure that τ_e is proportional to V^2, and that the 2D analytical solutions are four to five times larger than the 3D FE ones. Such a significant difference may be caused by neglecting electrical leakage in the 2D analytical solution. Considering that τ_e^0 = 0.42 x 10^{-9} Nm is necessary to start rotating the rotor as given in section 4.1, it is obvious from 〈Fig 14〉 that a driving voltage exceeding 170 V is indispensable in this configuration and sizes of the actuator.

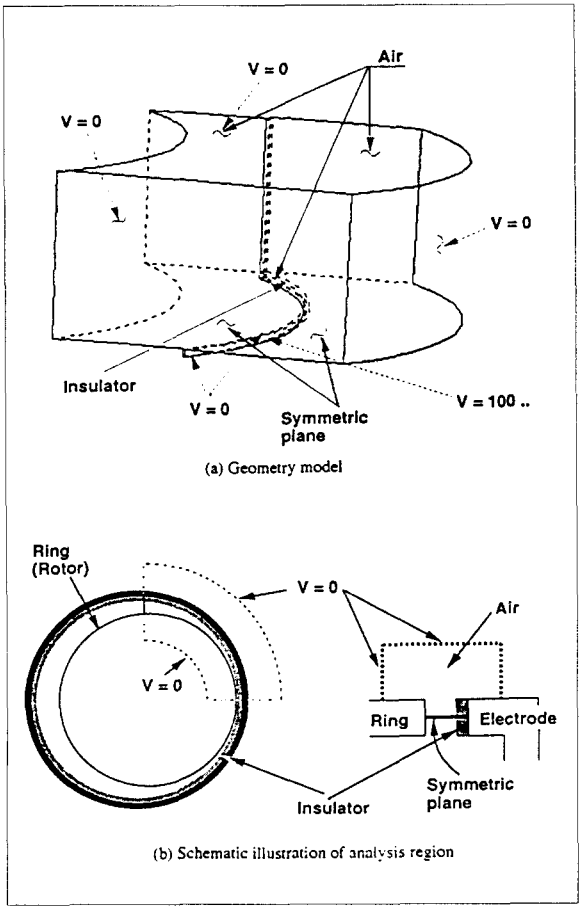

〈Fig 12〉 Geometry model and boundary conditions for air gap betweem rotor and one of electrodes

4.5 Recovery Process of Rotated Rotor

When the rotor is deformed to a certain extent and the voltage is disconnected, the deformed rotor is recovered dynamically. During this recovery process, the rotor should not touch any electrodes around itself. To ensure this, the dynamic response of the rotor deformed till ϕ=62 degrees, i.e. the elastic limit, is analyzed. It is found from the analysis that the rotor does not touch any of electrodes.

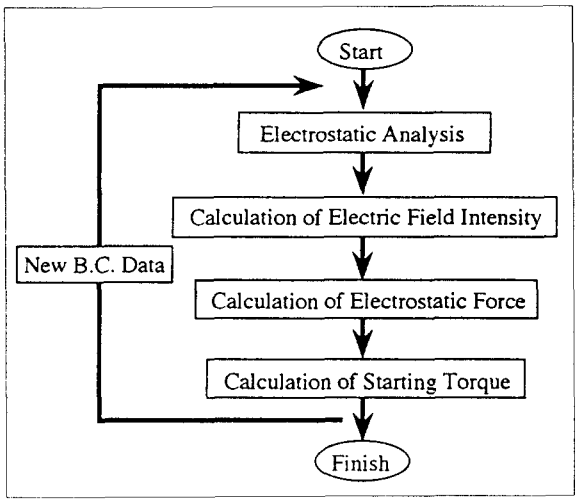

〈Fig 13〉 Flow chart of the electrostatic analysis

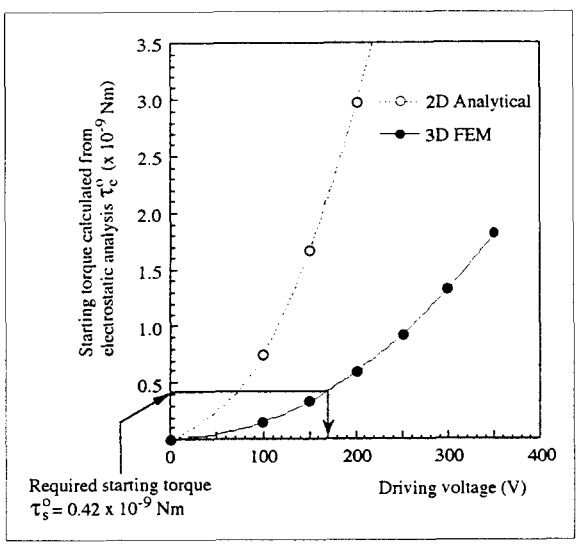

〈Fig 14〉 Calculated starting torque vs. driving voltage

4.6 Processing Speed

Generally, to do analysis and design work, various general purpose programs such as I-DEAS, Pro/Engineer, MARC and so on have been used. Using these programs, however,

conventional analyses of practical structures are still labour-intensive and are not easy for ordinary designers and engineers to perform.

〈Fig 15〉 summarized the measured processing time of a whole process plotted against all the analyses performed. These were measured on one of popular engineering workstations, SUN SPARCstation 10 (1CPU, 50MHz). In the electrostatic analysis, it takes about 15 minutes to perform all interactive operations, i.e. the definition of the geometry model shown in 〈Fig 12〉, the designation of local node patterns, and the assignment of material properties and boundary conditions. Node and element generations and the FE analysis are fully automatically performed in about 35 minutes.

In the analysis of in-plane deformation of the rotor, it takes about 40 minutes to perform interactive operations including solid modeling shown in 〈Fig 6〉, while about 70 minutes to fully automatically perform node and element generations and the FE analysis. In all the analyses, the designation of local node patterns and the assignment of material properties and boundary conditions take only about 20 seconds. Thus, the developed simulation system enables designers to easily evaluate detailed physical behaviors of micromachines through some simple interactive operations to their geometry models.

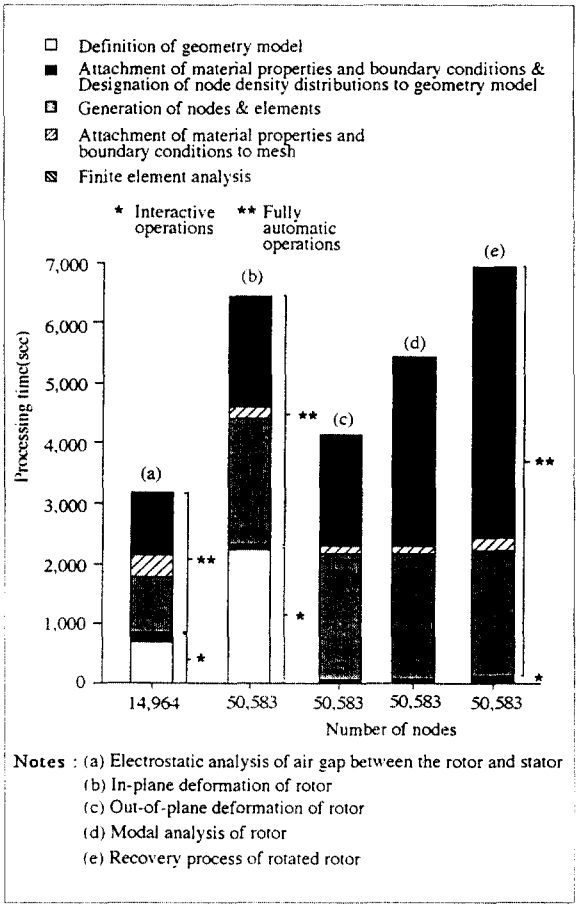

Notes : (a) Electrostatic analysis of air gap between the rotor and stator
(b) In-plane deformation of rotor
(c) Out-of-plane deformation of rotor
(d) Modal analysis of rotor
(e) Recovery process of rotated rotor

〈Fig 15〉 Processing times of various FE analyses

5. Conclusions

A new simulation system for micromachines was developed in the present study. This system was applied to the evaluation of practical behaviors of a micro wobble actuator. The conclusions given in the present paper can be summarized as follows.

Static and dynamic deformation, vibration and electrostatic behaviors of the micro wobble actuator were effectively evaluated in an easy and consistent manner using the developed system. Interactive operations to be done by an user can be performed in a reasonably short time. All the other processes which are time-consuming and labour-intensive in conventional systems can be automatically performed in a popular engineering workstation environment.

The micro wobble actuator considered in the present paper will be used as a micro positioning device in the near future.

References

[1] N. Nakajima, "Micromachines as Intelligent Artifacts", Proc. 1st Int. Symp. on Research into Artifacts, Tokyo, Japan, (1993), pp.48-51.

[2] K.W. Lee and K.D. Wise, "SENSIM : A Simulation Program for Solid-State Pressure Sensors", IEEE Transactions on Electron Devices, ED-29, (1982), pp.34-41.

[3] K. Nabors, S. Kim, J. White and S. Senturia, FastCap User's Guide, Research Laboratory of Electronics, Dept. of Electrical Engineering and Computer Science, MIT, Cambridge, MA 02139, U.S.A.

[4] J.R. Gilbert et al., "Implementation of a MEMCAD System for Electrostatic and Mechanical Analysis of Complex Structures from Mask Descriptions", Proceedings of the IEEE Micro Electro Mechanical Systems Workshop, Fort Lauderdale, (1993), pp.207-212.

[5] S. Crary, O. Juma and Y. Zhang, "Software Tools for Designers of Sensor and Actuator CAE Systems", IEEE Solid-State Sensors and Actuators (Transducers '91), San Francisco, CA, U.S.A., (1991), pp.498-501.

[6] Joon-Seong Lee et al., "Automatic Mesh Generation for Three-Dimensional Structures Consisting of Free-Form Surfaces", Journal of the Korea Society of CAD/CAM Engineers, Accepted for publication, 1996.

[7] MARC Analysis Research Corporation, MARC manual k5.2, 1994.

[8] H. Chiyokura, Solid Modeling with Designbase : Theory and Implementation, Adison-Wesley, 1988.

[9] N. Shibaike, "Design of Micro-mechanisms Focusing on Configuration", Materials and Processes, Materials & Design, To appear.

[10] L.A. Zadeh, "Fuzzy Algorithms", Information and Control, Vol. 12, (1968), pp.94-102

[11] L.A. Zadeh, "Outline of a New Approach to the Analysis of Complex Systems and Decision Process", IEEE Transactions on Systems, Man and Cybernetics, SMC-3, (1973), pp.28-44.

[12] T. Asano, "Practical Use of Bucketing Techniques in Computational Geometry", Computational Geometry, North-Holland, (1985), pp.153-195.

[13] D.F. Watson, "Computing the n-Dimensional Delaunay Tessellation with Application to Voronoi Polytopes", The Computer Journal, Vol. 24, (1981), pp.162-172.

[14] S.W. Sloan, "A Fast Algorithm for Constructing Delaunay Triangulation in the Plane", Advances in Engineering Software, Vol. 9, (1987), pp.162-172.

[15] O.D. Jefimenko, Electrostatic Motors, Electret Science, Company, Star City, 1973.

[16] W.S.N. Trimmer, "Microrobots and Micromechanical Systems", Sensors and Actuators A, Vol. 19, (1989), pp.267-287.

[17] H. Fujita and A. Omodaka, "The Principle of an Electrostatic Linear Actuator Manufactured by Silicon Micromachining", IEEE Solid-State Sensors and Actuators (Transducers '87), Tokyo, Japan, 1987, pp.861-864.

[18] Y.C. Tai, L.S. Fan and R.S. Muller, "IC-Processed Micro-Motors : Design, Technology, and Testing", Proceedings of the 2nd IEEE Workshop on Micro Electro Mechanical Systems(MEMS), Salt Lake City, UT, U.S.A., 1989, pp.1-6.

[19] T. Hirano, T. Furuhata, K.J.Gabriel and H. Fujita, "Design, Fabrication, and Operation of Submicron Gap Comb-Drive Microactuators", Journal of Microelectromechanical Systems, Vol. 1, No. 1, (1992), pp.52-59.

[20] M.P. Omar and R.L. Mullen, "Electric and Fluid Analysis of Side-Drive Micromotors", Journal of Microelectromechanical Systems, Vol. 1, Nol. 3, (1992), pp.130-140.

[21] Y.C. Tai and R.S. Muller, "IC-processed Electrostatic Synchronous Micromotors", Sensors and Actuators A, Vol. 20, (1989), pp.49-55.

[22] H. Fujita and A. Omodaka, "The Fabrication of an Electrostatic Linear Actuator by Silicon Micromachining", IEEE Transactions on Electron Devices, Vol. 35, No. 6, (1988), pp.731-734.

[23] J.S. Lee et al., "A CAE System for Micromachines : Its Application to Electrostatic Micro Wobble Actuators" Sensors and Actuators A, Accepted for Publication, 1996.

● 저자소개 ●

이준성
1986년 성균관대학교 기계공학과 학사
1988년 동대학원 기계공학과 석사
1988년-1991년 육군사관학교 기계공학과 전임
1991년-1992년 KIST 기전연구부 연구원
1995년 동경대학교 대학원 공학계 연구과 공학박사
현 재 경기대학교 기계공학과 전임.
관심분야 : CAE, 구조물의 자동설계, 마이크로머쉰의 설계